

# UC Davis

## UC Davis Previously Published Works

### Title

Initiation of Chondrocyte Self-Assembly Requires an Intact Cytoskeletal Network.

### Permalink

<https://escholarship.org/uc/item/4jm7f82c>

### Journal

Tissue engineering. Part A, 22(3-4)

### ISSN

1937-3341

### Authors

Lee, Jennifer K  
Hu, Jerry CY  
Yamada, Soichiro  
et al.

### Publication Date

2016-02-01

### DOI

10.1089/ten.tea.2015.0491

Peer reviewed

**ORIGINAL ARTICLE**

---

# Initiation of Chondrocyte Self-Assembly Requires an Intact Cytoskeletal Network

Jennifer K. Lee, PhD,<sup>1</sup> Jerry C.Y. Hu, PhD,<sup>1</sup> Soichiro Yamada, PhD,<sup>1</sup> and Kyriacos A. Athanasiou, PhD, PE<sup>1,2</sup>

Self-assembly and self-organization have recently emerged as robust scaffold-free tissue engineering methodologies that can be used to generate various tissues, including cartilage, vessel, and liver. Self-assembly, in particular, is a scaffold-free platform for tissue engineering that does not require the input of exogenous energy to the system. Although self-assembly can generate functional tissues, most notably neocartilage, the mechanisms of self-assembly remain unclear. To study the self-assembling process, we used articular chondrocytes as a model to identify parameters that can affect this process. Specifically, the roles of cell–cell and cell–matrix adhesion molecules, surface-bound collagen, and the actin cytoskeletal network were investigated. Using time-lapse imaging, we analyzed the early stages of chondrocyte self-assembly. Within hours, chondrocytes rapidly coalesced into cell clusters before compacting to form tight cellular structures. Chondrocyte self-assembly was found to depend primarily on integrin function and secondarily on cadherin function. In addition, actin or myosin II inhibitors prevented chondrocyte self-assembly, suggesting that cell adhesion alone is not sufficient, but rather the active contractile actin cytoskeleton is essential for proper chondrocyte self-assembly and the formation of neocartilage. Better understanding of the self-assembly mechanisms allows for the rational modulation of this process toward generating neocartilages with improved properties. These findings are germane to understanding self-assembly, an emerging platform for tissue engineering of a plethora of tissues, especially as these neotissues are poised for translation.

## Introduction

**T**RADITIONAL TISSUE ENGINEERING approaches combine a cell source with an exogenous scaffold and chemical or mechanical stimulation regimens. This paradigm can be applied to a wide variety of engineered tissues, from bone to skin to cardiac muscle. Recently, the emergence of scaffold-free approaches has demonstrated significant benefits in certain target tissues. These scaffold-free approaches can be divided into the self-assembling and self-organization processes, which have been applied to numerous tissues, including the liver, kidney, cartilage, ligament, and vascular.<sup>1,2</sup> The self-assembling process is distinct from self-organization, in that it does not require the addition of exogenous energy to the system. Self-assembly is especially beneficial for engineering of cartilages of the body, including hyaline articular cartilage,<sup>3</sup> meniscal fibrocartilage,<sup>4</sup> and fibrocartilage of the temporomandibular joint.<sup>5</sup>

Tissue engineering using the scaffold-free approach of self-assembly has been most validated in the study of articular cartilage.<sup>6</sup> Note that self-assembly of chondrocytes is distinct from chondrocyte aggregation, in that self-assembly

generates large clinically relevant sized tissues, whereas chondrocyte aggregation does not. The detailed mechanism by which chondrocytes assemble into functional cartilage tissue is not well understood. Mechanistic understanding of chondrocyte self-assembly will guide more rational selection of exogenous chemical and mechanical regimens to increase the tissue's functional properties. Ultimately, self-assembly of articular cartilage aims to replace damaged tissues resulting from trauma or degeneration. If left untreated, degeneration leads to osteoarthritis, which affects over 240 million individuals worldwide.<sup>7</sup> Treatment options include microfracture, mosaicplasty, and autologous chondrocyte implantation. These techniques aim to restore tissue function, but can result in inferior fibrocartilage formation and donor site morbidity. Total joint replacements mimic the natural motion of the joint, but are end-stage options that remove significant portions of healthy bone and cartilage. Tissue engineering, self-assembly in particular, has emerged as an intermediate treatment option that restores joint function by forming mechanically robust neocartilage.

The first key step in chondrocyte self-assembly as well as aggregation is cell–cell or cell–matrix adhesion. During

---

Departments of <sup>1</sup>Biomedical Engineering and <sup>2</sup>Orthopedic Surgery, University of California, Davis, Davis, California.

chondrocyte self-assembly, N-cadherin labeling of neocartilage 1 day post-tissue formation increased,<sup>8</sup> suggesting that self-assembly is mediated by N-cadherin. This is consistent with the role of N-cadherin during mesenchymal condensation during cartilage development.<sup>9,10</sup> In addition, inhibition of integrin-collagen binding significantly reduced the ability of chondrocytes to aggregate in culture.<sup>11</sup> Furthermore, collagenase, in addition to  $\beta 1$  integrin antibody, reduced chick chondrocyte aggregation.<sup>12,13</sup> Collectively, these studies demonstrate that both cadherins and integrins may play a role in chondrocyte aggregation and in the self-assembling process. However, the mechanism by which chondrocytes self-assemble remains to be fully elucidated.

Motivated by the work in chondrocyte aggregation and our early work investigating the self-assembling process, we sought to elucidate the roles of cadherin, integrin, and collagen in chondrocyte self-assembly toward establishing the relative contributions of cell-cell versus cell-matrix interactions. Moreover, this study aimed to determine the effect of surface-bound collagen on chondrocyte self-assembly. Removal of surface-bound collagen is hypothesized to not influence the properties of self-assembled neocartilage. Finally, to move beyond cell surface interactions (i.e., via cadherin, integrin, and surface-bound collagen), we sought to explore the coordination of intracellular cytoskeletal events, involving the myosin-actin network, and their effect on self-assembly. It was hypothesized that (i) cadherins and integrins have distinct roles in the self-assembling process and that (ii) coordination of the intracellular milieu—specifically, cytoskeletal elements—promotes robust self-assembly.

## Materials and Methods

### *Chondrocyte isolation*

Articular cartilage was obtained from the distal femur of juvenile bovine joints (Research 87). Collagenase type II (0.2%) (Worthington) was used to digest the tissue for 18 h. Cells were washed in 1% penicillin-streptomycin-fungizone (PSF; Lonza BioWhittaker) in Dulbecco's modified Eagle's medium (DMEM) before freezing in 10% dimethyl sulfoxide and 20% fetal bovine serum (FBS) medium. Cells were stored at  $-80^{\circ}\text{C}$  until they were used in experiments.

### *Chondrocyte self-assembly*

Chondrocytes were thawed rapidly in a warm water bath and rinsed thrice with 1% PSF in DMEM before resuspension in chondrogenic (CHG) medium consisting of DMEM with GlutaMAX (Gibco); 0.1 mM nonessential amino acids (Gibco); 1% ITS+ (insulin, human transferrin, and selenous acid; BD Biosciences); 1% PSF; 100 nM dexamethasone (Sigma); 50  $\mu\text{g}/\text{mL}$  ascorbate-2-phosphate (Sigma); 100  $\mu\text{g}/\text{mL}$  sodium pyruvate (Sigma), and 40  $\mu\text{g}/\text{mL}$  L-proline (Sigma). To each segment of a quad Petri dish (Greiner), 4 M cells in 100  $\mu\text{L}$  chondrogenic medium (+experimental conditions) were added. Up to four experimental conditions were examined simultaneously. To test the effects of cell-matrix interactions and cytoskeletal elements, each of the following was resuspended in CHG medium: EDTA (5  $\mu\text{M}$ ), EGTA (5  $\mu\text{M}$ ), 0.2% collagenase+3% FBS, cytochalasin D (2  $\mu\text{M}$ ), blebbistatin (50  $\mu\text{M}$ ), and Y27632 (50  $\mu\text{M}$ ) (unless otherwise noted; Sigma).

Because collagenase pretreatment did not affect self-assembly in our time-lapse experiments, we could assess the impact of removing surface-bound collagen on neocartilage properties. Agarose (2% wt/vol in phosphate-buffered saline [PBS]) wells, 5 mm in diameter, were prepared as described previously<sup>14</sup>; PBS was exchanged with CHG at least thrice. After thawing, cells were washed in 1% PSF in DMEM before resuspending in CHG (control group), CHG +3% FBS (FBS control group), or CHG +0.2% collagenase +3% FBS (CGN group) for 1.5 h. Cells were resuspended in CHG before seeding at 4.5 M cells in 100  $\mu\text{L}$  CHG per agarose well. After 4 h, neocartilage was supplemented with additional CHG. At day 12, neocartilage was assessed mechanically, biochemically, and histologically as previously described.<sup>14</sup> Briefly, the creep indentation compressive test and the strain-to-failure tensile test were used to determine the compressive and tensile properties of engineered neocartilage, respectively. For creep indentation testing, a 0.8 mm diameter flat, porous indenter tip was applied to the sample under a 0.3 or 0.5 g mass to achieve tissue strains of 3–5%. The time-displacement curve was analyzed using a semianalytical, seminumeric, linear biphasic model to determine the aggregate modulus, a measure of compressive stiffness, the permeability, and the Poisson's ratio.<sup>15</sup> The strain-to-failure tensile test applied a strain rate of 1% of the gauge length to dog bone-shaped specimens until the sample failed. The generated load-displacement curve was normalized to a stress-strain curve from which the Young's modulus, a measure of tensile stiffness, and the ultimate tensile strength were determined from the slope of the curve and the peak load achieved, respectively.

### *Microscopy and time-lapse analysis*

Cells were imaged using a Zeiss AxioObserver equipped with a Yokogawa CSU-10 spinning disk confocal system, 40 $\times$  or 10 $\times$  objectives, 488 and 561 nm solid-state lasers, an ASI motorized microscope stage, and a Photometrics CoolSNAP HQ camera. The microscope system was controlled by Slidebook software (Intelligent Imaging Innovations). For live cell imaging, the temperature was set to 37 $^{\circ}\text{C}$  by a custom microscope heating chamber. Bright-field images using differential interference contrast (DIC) optics were taken every 10 min to visualize the rate and degree of self-assembly.  $N=4-6$  regions were imaged per condition. Representative time-lapse videos for each condition are provided as Supplementary Videos S1–S9 (Supplementary Data are available online at [www.liebertpub.com/tea](http://www.liebertpub.com/tea)).

Each time-lapse video was processed in ImageJ (National Institutes of Health, Bethesda, MD) to assess the degree of self-assembly. Initially, cells were well dispersed in the field of view with minimal void spaces among cells. As cells self-assembled into clusters and compacted into tight cell colonies, void spaces among cells increased, and accordingly, local, projected cell density increased. Once the cells formed tight colonies, the cell-cell boundary was not readily discriminated; therefore, the direct quantification of cell density within cell clusters was impossible. Instead, we quantified this void space using a combination of image processing functions to exaggerate the cell boundaries. DIC images were processed using Band Pass Filter, Find Edge, and Gaussian Blur functions in ImageJ, then thresholded to

select the void space among cell clusters. Assuming that the number of cells in the field of view stays constant during the experiments (we observed minimal cell division in our experiments), we calculated the cell density by taking the initial cell number per field of view and dividing this number by the area occupied by cells, which was derived from the void space measured from each frame. The self-assembly index was defined as  $[c(t) - c_{min}] / [c_{max} - c_{min}]$  where  $c(t)$  is the projected cell density at any given time point,  $c_{min}$  is the minimal cell density, and  $c_{max}$  is the maximum cell density.  $c_{min}$  is observed immediately after cell seeding and  $c_{max}$  is observed when the self-assembled neocartilage reaches a steady state. The control condition reached  $c_{max} \sim 4$  h after seeding. To compare different treatment regimens, the  $c_{max}$  from the control was used for all conditions within the experiment. Dotted outlines approximating chondrocyte self-assembly are provided in Figures 1–4.

#### Immunofluorescence staining

Chondrocytes were seeded onto collagen type I-coated coverslips for 72 h. Cells were formalin fixed and stained with phalloidin, a marker for F-actin, and antibody to collagen type II (Cedar Lane). Cells were imaged using a spinning disc confocal microscope (Intelligent Imaging Innovations).

#### Western blot analysis

Neocartilage constructs self-assembled under continuous treatment with various inhibitors (as in time-lapse imaging) were prepared for Western blot analysis. Constructs were homogenized in sample buffer containing 5%  $\beta$ -mercaptoethanol at 0, 2, 6, 12, 24, 48, and 72 h. The samples were run using a standard sodium dodecyl sulfate–polyacrylamide gel electrophoresis (SDS-PAGE) system (Bio-Rad) and transferred to nitrocellulose membranes. The primary antibodies used were collagen type II (Cedar Lane), collagen type VI (Abcam), N-cadherin (BD Biosciences), or  $\beta$ -tubulin (Sigma). The secondary antibodies were either anti-mouse or rabbit conjugated with horseradish peroxidase (HRP; Jackson laboratory). Blots were developed using the WesternBright ECL HRP substrate kit (Advansta, Inc.) and imaged with a Bio-Rad imager.

#### Statistical analyses

JMP 9.0.1 (SAS Institute) was used to perform statistical analyses. One-way ANOVA was used to assess differences among groups in the self-assembling tissue engineering process, followed by Tukey's *post hoc* test ( $p < 0.05$ ). An  $n = 5-7$  was used. Groups not connected by the same symbol are statistically significant, and data are represented as mean  $\pm$  standard deviation.

## Results

By using a time-lapse experimental method in a 35-mm glass bottom dish with a quadrant divider, we visualized chondrocytes in various conditions using a fully automated live cell microscope (Fig. 1A). Initially, chondrocytes were well dispersed as single cells or as a few cell clusters (Fig. 1B,

0 h); however, these cells, while undergoing thermal fluctuations, rapidly initiated cell-to-cell contacts before condensing into larger cell clusters (Fig. 1B and Supplementary Video S1). As self-assembly progressed, cell-to-cell boundaries among chondrocytes were difficult to distinguish as cells tightly adhered to each other and compacted (Fig. 1B, 6 h). Self-assembly of chondrocytes reached an apparent steady state around 4 h postseeding; this steady state was confirmed by the quantification of the self-assembling process (Fig. 1C). Immunofluorescence imaging of chondrocyte clusters showed that cells are filled with collagen II and are surrounded by a collagen network (Fig. 1D), indicating that cells also establish cell–extracellular adhesions during the self-assembling process.

Based on the live cell imaging analysis, at a macroscopic level, the cell–cell interactions of chondrocytes appear to initiate the self-assembling process. To tease out the potential roles of cell–cell versus cell–extracellular matrix interactions, the chondrocyte suspensions were treated with EGTA and EDTA that chelate primarily  $Ca^{2+}$  and  $Ca^{2+}/Mg^{2+}$ , respectively. Both EGTA and EDTA chelate calcium that is required for calcium-dependent, cadherin-mediated cell–cell adhesion. EDTA also binds to magnesium. EGTA, on the other hand, binds only weakly to magnesium, known to be a primary mediator of integrin function.<sup>16</sup> Interestingly, chondrocytes treated with EGTA assembled similarly to the control condition, but chondrocytes treated with EDTA did not (Fig. 2A, B). This result indicates that disruption of cadherin-mediated cell–cell adhesion (via EGTA) alone is not sufficient to inhibit chondrocyte self-assembly. Coupled with the lack of efficient chondrocyte self-assembly in the presence of EDTA, this result shows that intact integrin function is the primary mediator of self-assembly.

To test the roles of collagens in chondrocyte self-assembly, we first analyzed the level of collagen II during chondrocyte self-assembly. The procollagen molecule (the higher molecular weight band in Fig. 3A) was detected in chondrocytes and gradually increased in expression. Final processing of the procollagen through both N- and C-terminal cleavage yields the mature collagen type II, which started to appear 6–8 h after seeding (the lower molecular weight bands denoted by the arrow in Fig. 3A and see also Fig. 3B). This result demonstrates that chondrocytes increased the level of mature collagen II during self-assembly by completing collagen processing. Note that the level of N-cadherin, a predominant cadherin in chondrocytes, stayed relatively constant (Fig. 3A).

Isolation of chondrocytes requires extensive enzymatic digestion of the collagen network, and collagenase treatment may not completely remove the existing collagen network. Thus, to investigate the role of residual surface-bound collagen fragments on the surface of isolated chondrocytes, an additional collagenase digestion step was used on cells before time-lapse imaging and traditional self-assembly. Treatment with collagenase significantly reduced the levels of both collagen II and VI (Fig. 3B). However, these collagenase-pretreated chondrocytes assembled tight cell clusters similar to the cells in the control (Fig. 3C, D). This difference in protein expression may be simply due to incomplete collagen digestion (see the presence of residual collagen II and VI in Fig. 3B) and that this residual amount

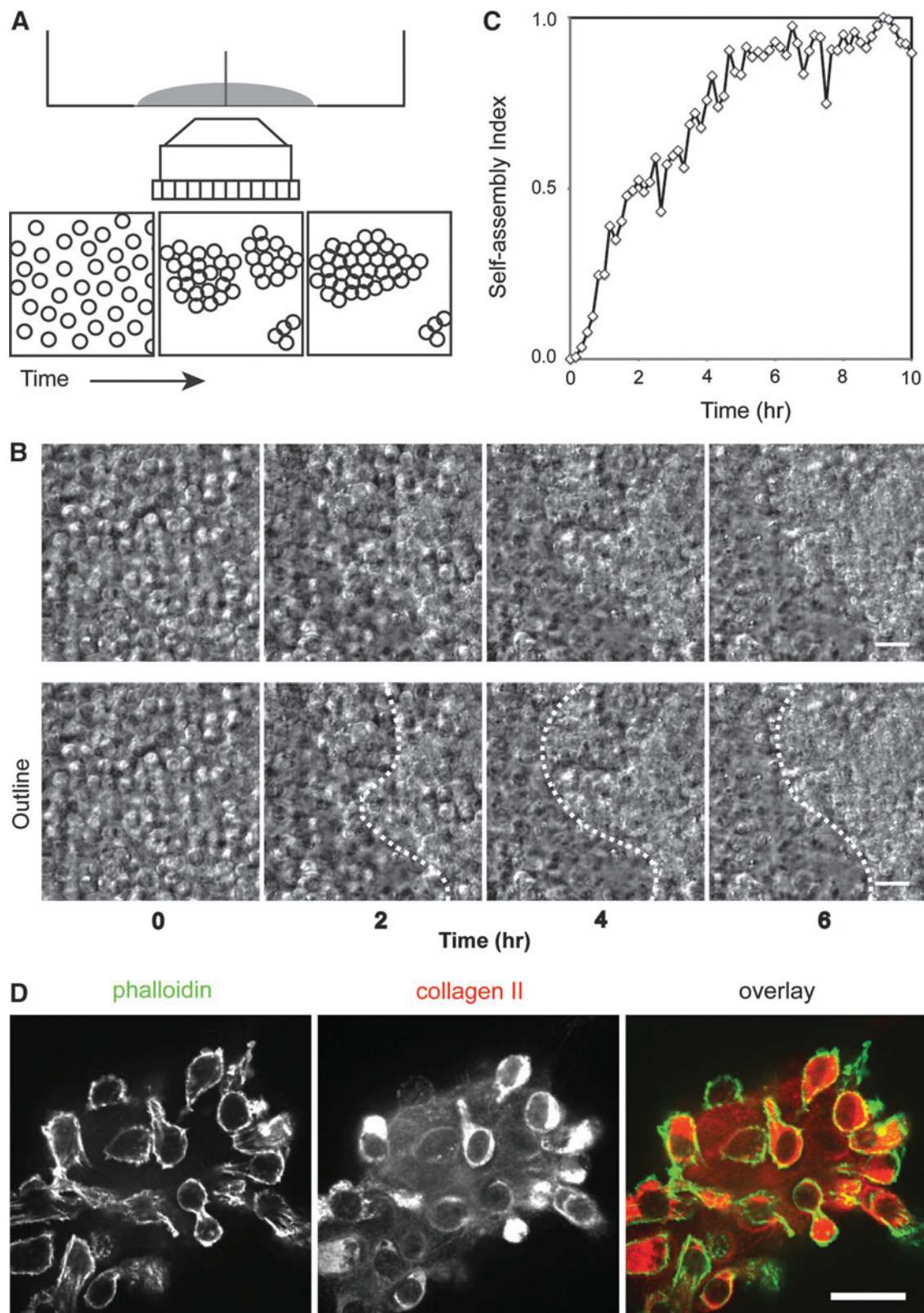


**FIG. 1.** Analysis of the self-assembling process. **(A)** Schematic of experimental setting. Time-lapse microscopy was used to visualize and assess the effects of various conditions on the degree of self-assembly over time. **(B)** Live chondrocytes imaged with differential interference contrast (DIC) optics. Initially, cells are well dispersed, but rapidly congregate and condense into compact cell clusters. Time in hours. Scale bar 20  $\mu\text{m}$ . **(C)** An example of quantification of the self-assembling process. In general, self-assembly in control conditions reaches a steady state  $\sim 4$  h after seeding. See the Materials and Methods section for the details of calculation of the self-assembly index. **(D)** Immunofluorescence of a chondrocyte cluster cultured on collagen type I-coated coverslips 3 days after seeding. Chondrocytes exhibit a rounded morphology, with robust production and secretion of collagen type II among cells. Scale bar 20  $\mu\text{m}$ . Color images available online at [www.liebertpub.com/tea](http://www.liebertpub.com/tea)



**FIG. 2.** EDTA inhibits self-assembly, but EGTA does not. **(A)** Time-lapse experiments assessing EDTA and EGTA compared with control conditions reveal significant impairment of self-assembly with EDTA. Scale bar 20  $\mu$ m. **(B)** Quantification of the self-assembling process. While the presence of EGTA (when primarily cadherin is blocked) does not inhibit chondrocyte self-assembly, chondrocytes cannot self-assemble in the presence of EDTA (when both integrin function and cadherin function are blocked).

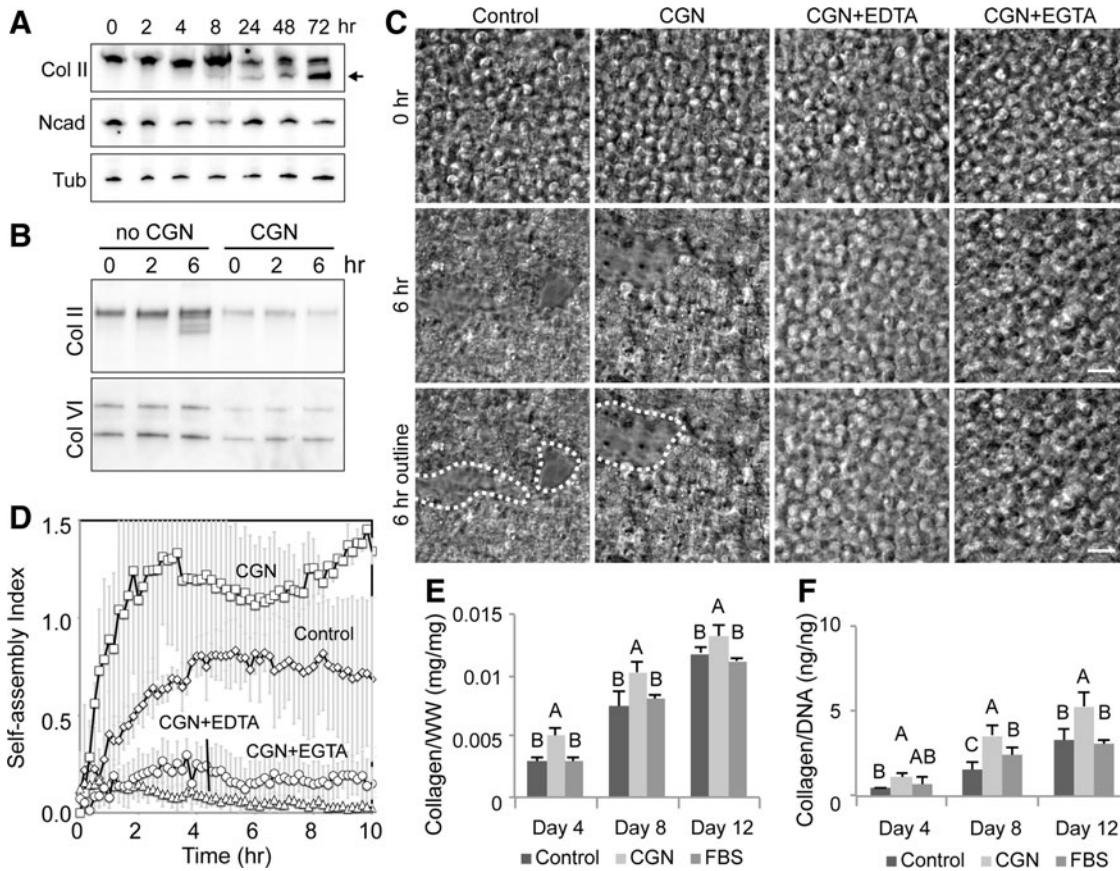
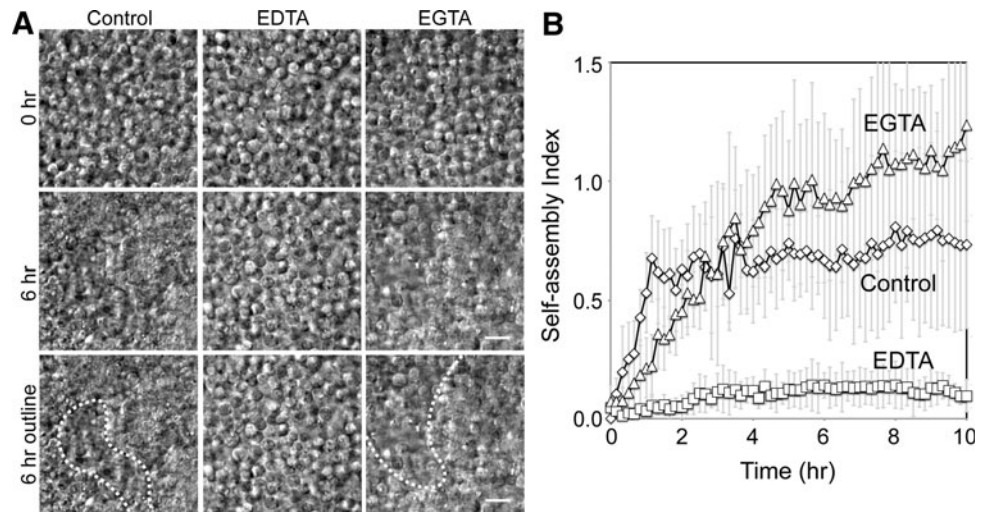


**FIG. 3.** The role of collagen in chondrocyte self-assembly. **(A)** Western blot analysis of chondrocytes during self-assembly. The precursor of collagen II (Col II, higher molecular weight band at the top of the lane) is abundant in chondrocytes. The processed form of collagen II (smaller molecular weight bands indicated by the arrow) becomes detectable at 8 h after seeding. N-cadherin (Ncad) levels stay relatively constant during the initial stages of self-assembly. Tubulin (Tub) is used as a loading control. **(B)** The addition of a collagenase pretreatment decreases both collagen II and VI levels. **(C)** DIC images of chondrocyte self-assembly in the presence of collagenase (CGN), CGN+EDTA, or CGN+EGTA. Scale bar 20  $\mu$ m. **(D)** Quantification of the self-assembling process. While collagenase alone is not sufficient to inhibit chondrocyte self-assembly, the presence of EDTA or EGTA with collagenase pretreatment significantly reduces self-assembly. **(E)** Treatment with collagenase resulted in significant increases in collagen production when normalized to wet weight of tissue. **(F)** Collagenase treatment significantly increased collagen production per cell. Groups not connected by the same letters in **(E, F)** are statistically significant.

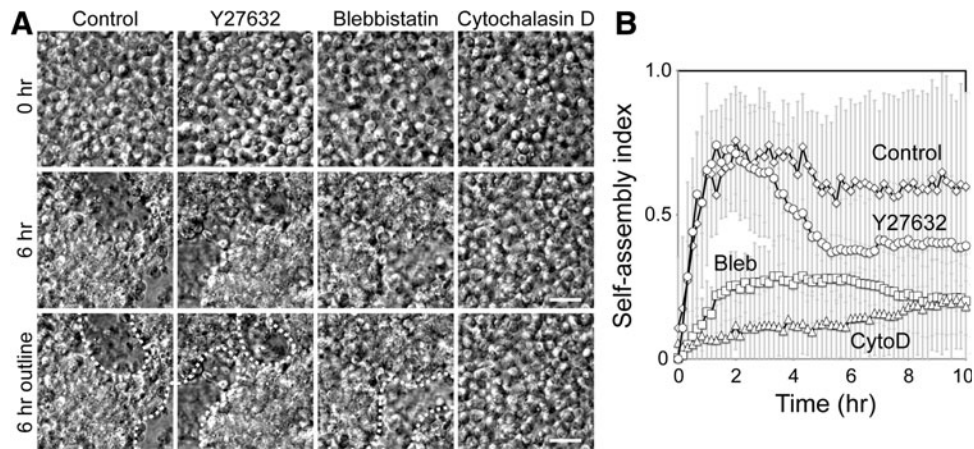


**FIG. 4.** Intact cytoskeleton is required for efficient chondrocyte self-assembly. **(A)** DIC images of chondrocytes in the presence of pharmacological agents inhibiting ROCK (Y27632), myosin (blebbistatin), and actin (cytochalasin D). Scale bar 20  $\mu\text{m}$ . **(B)** Quantification of self-assembly in the presence of pharmacological agents. Both blebbistatin and Y27632, an inhibitor of the myosin II pathway, compromise the self-assembling process, while cytochalasin D, an actin-disrupting drug, is most effective in reducing chondrocyte self-assembly.

of surface-bound collagens still is sufficient for chondrocyte self-assembly. Alternatively, in the absence of intact collagen networks, cell–cell adhesion may be sufficient to mediate self-assembly. Interestingly, when chondrocytes were treated with both collagenase and EDTA (CGN+EDTA) or collagenase and EGTA (CGN+EGTA), effectively eliminating both integrin and cadherin function, self-assembly was significantly reduced (Fig. 3C, D). Unlike EGTA treatment alone where chondrocytes efficiently self-assembled (Fig. 2A, B), significant inhibition of chondrocyte self-assembly in CGN+EGTA-treated cells supports the notion that in the absence of a collagen network, cadherin plays a role in the self-assembling process. Cadherin is thus a secondary mediator of the self-assembling process.

To examine the long-term effects of removing residual surface-bound collagen fibers from the cellular surface, collagenase-treated cells were placed in traditional self-assembly. After 4, 8, and 12 days, we assessed the biochemical and mechanical properties of neocartilage. Functional properties were not significantly different between controls and collagenase-treated groups (compressive stiffness of  $156 \pm 32$  kPa versus  $164 \pm 54$  kPa ( $p > 0.12$ ), respectively, and tensile stiffness of  $1.39 \pm 0.39$  MPa versus  $1.12 \pm 0.11$  MPa ( $p > 0.76$ ), respectively). We detected a significant change in collagen production per cell in collagenase-pretreated neocartilage compared with both the FBS and standard controls. The removal of extracellular collagen, thus, initiated increased cellular synthesis of collagen, detectable at each time point assessed.

Since chondrocytes tightly compacted during self-assembly, suggesting that intracellular forces drive cellular clustering, we sought to test the role of the actin cytoskeleton. The actin cytoskeleton, together with force-generating myosin II, provides an important intracellular structure to strengthen cell–cell interactions. Treatment with Y27632, a ROCK inhibitor (ROCK is an upstream regulator of myosin II), or blebbistatin, a myosin II inhibitor, reduced chondrocyte self-assembly (Fig. 4A). Interestingly, ROCK inhibition did not prevent the initial self-assembly, but, after several hours, these cells failed to compact fully (Fig. 4B).

These results indicate that the activity of myosin II is required for chondrocyte self-assembly. Furthermore, treatment with cytochalasin D, an actin-capping molecule that disrupts actin network dynamics in live cells, significantly reduced self-assembly (Fig. 4A, B). While the initial cell adhesion (whether cell–cell or cell–matrix mediated) is critical for the initiation of self-assembly, our analysis demonstrated an important role of the actin cytoskeleton during the self-assembly of chondrocytes.

## Discussion

The self-assembling process is a robust, scaffold-free tissue engineering technique that is used to engineer neocartilages with functional properties. Although chondrocyte self-assembly is thought to mimic the stages of chondrogenesis, the initial key steps of self-assembly have not been characterized in detail. The early stages of chondrocyte self-assembly impact the formation of neocartilage in a process akin to mesenchymal condensation during chondrogenesis. Our approach combines live cell imaging with an established protocol of chondrocyte self-assembly to directly visualize *de novo* chondrocyte self-assembly, cell–cell and cell–matrix interactions mediated through cadherins and integrins, respectively, promote the initial cell contacts, followed by compaction of cells into dense cellular structures. EDTA treatment reduces chondrocyte self-assembly, while EGTA does not (Fig. 2), indicating that integrins alone can facilitate self-assembly. However, in the absence of collagen (via pretreatment of chondrocytes with collagenase), chondrocytes nonetheless assemble into robust clusters (Fig. 3C, D), suggesting that in the absence of collagen, cadherin-mediated cell–cell adhesion likely plays a dominant role. This finding is consistent with the upregulation of N-cadherin and NCAM in mesenchymal cell condensation that precedes chondrogenesis<sup>9,10</sup> and the N-cadherin localization seen during the early stages of chondrocyte self-assembly.<sup>8</sup> Our results suggest that self-

assembly is primarily mediated by integrin-matrix binding in the presence of collagen, but secondarily mediated by cadherin function in the absence of collagen.

It is important to note that cell surface-associated molecules may influence the cell-cell or cell-matrix interactions during the self-assembling process or as demonstrated in previous chondrocyte aggregation studies.<sup>11</sup> Primary chondrocytes used in the self-assembling process are harvested from the dense articular cartilage of juvenile bovine knees through digestion in collagenase overnight<sup>8</sup>; the resulting digestion is a viscous slurry of cells, matrix, and collagenase. As the collagens are released from the cartilage tissue, collagenase enzyme can be bound by these liberated molecules, reducing enzyme activity elsewhere (i.e., at the remaining tissue fragments or at the cell surface). Residual collagen bound to the cell surface may not be fully digested and may ultimately contribute to chondrocyte clustering, especially in self-assembly where high cell concentrations are often used. This excess collagen may preferentially drive cell-matrix versus cell-cell interactions. The possibility of integrin- and collagen-driven self-assembly motivated our studies of collagenase pretreatment of cells. Prior studies that sought to determine whether cells primarily use cadherin or integrin to mediate aggregation or self-assembly may have been impacted by residual collagen fragments at the cell surface.

Chondrocytes are generally rounded in morphology and do not have an extensive actin stress fiber network often observed in other cell types. In fact, treatment with cytochalasin to disrupt the actin cytoskeleton has been used to promote the rounded chondrocytic phenotype and differentiation.<sup>17</sup> Cytochalasin treatment of dedifferentiated chondrocytes stimulates a chondrogenic phenotype, including increased expression of collagen II<sup>18-20</sup> and Sox9<sup>18</sup> and synthesis of proteoglycan.<sup>21</sup> These results largely indicate that a morphology driven by diminished cytoskeletal tension is crucial to chondrogenesis and chondrocyte redifferentiation. In contrast, this study demonstrated that a functional actin network is important for robust self-assembly. Although the same concentration of cytochalasin D is used in these studies, cytochalasin D may be beneficial for the redifferentiation of cells that are expected to exhibit a stiffer more fibroblastic-like cytoskeleton, but disruptive to the self-assembly of primary chondrocytes. Indeed, the cell stiffness of stem cells has been shown to be higher than primary chondrocytes.<sup>22</sup> Thus, the impact of cytochalasin D is dependent on the differentiation status of cells.

Other mediators of the actin cytoskeletal network have also been shown to play crucial roles in chondrocyte differentiation and phenotype maintenance. ROCK inhibition, for example, upregulates Sox9 in chondrocytes.<sup>23</sup> Rac1 and Cdc42, upstream regulators of the actin network, have also been shown to upregulate N-cadherin and promote chondrogenesis.<sup>24</sup> Despite the importance of these cytoskeletal inhibitors on promoting chondrocyte morphology and differentiation, our results demonstrated that the intact actin cytoskeleton is essential for the self-assembly and proper formation of neocartilage. The inhibitors of actin, ROCK, and myosin II significantly reduced the initial self-assembly of chondrocytes (Fig. 4). These results suggest that the initial cell adhesion and subsequent cell compaction require a functional actin-myosin II network. While the suppression

of a robust actin network may artificially promote chondrogenesis by upregulation of chondrocyte markers, our results suggest that the intact actin-myosin II network is required for the assembly of chondrocytes into neocartilage.

Using techniques ranging from time-lapse imaging to scaffold-free tissue engineering, we analyzed cellular self-assembly to elucidate the mechanisms of the early stages of this process, using articular cartilage as the model. We demonstrated that rapid chondrocyte self-assembly depends primarily on cell-matrix adhesion and secondarily on cell-cell interactions. Our analysis also indicated that the actin cytoskeleton is critical to robust self-assembly. These early events likely dictate the ultimate properties of self-assembled neocartilage. Therefore, better understanding of this process may lead to the rational selection of agents that can influence the process and ultimately lead to increased neocartilage functional properties. Although this study focused on the self-assembly of articular chondrocytes, the mechanism of this process may also apply to alternative cell types. For example, cell adhesion and actin cytoskeleton likely regulate proper cell-to-cell arrangement in tissues with heterogeneous cell populations. Ultimately, an extensive understanding of the self-assembly mechanisms allows for the identification of novel methods to alter the process toward engineering of various neotissues.

#### Acknowledgments

This publication was made possible with support from the National Institutes of Health (R01 AR067821) and from the National Institute of General Medical Sciences (NIGMS) for J.K.L. (T32-GM00799) and S.Y. (R01 GM094798). Its contents are solely the responsibility of the authors and do not necessarily represent the official views of the NIH or NIGMS.

#### Disclosure Statement

No competing financial interests exist.

#### References

1. Athanasiou, K.A., Eswaramoorthy, R., Hadidi, P., and Hu, J.C. Self-organization and the self-assembling process in tissue engineering. *Annu Rev Biomed Eng* **15**, 115, 2013.
2. Huey, D.J., Hu, J.C., and Athanasiou, K.A. Unlike bone, cartilage regeneration remains elusive. *Science* **338**, 917, 2012.
3. Makris, E.A., Responde, D.J., Paschos, N.K., Hu, J.C., and Athanasiou, K.A. Developing functional musculoskeletal tissues through hypoxia and lysyl oxidase-induced collagen cross-linking. *Proc Natl Acad Sci U S A* **111**, E4832, 2014.
4. Huey, D.J., and Athanasiou, K.A. Alteration of the fibrocartilaginous nature of scaffoldless constructs formed from leporine meniscus cells and chondrocytes through manipulation of culture and processing conditions. *Cells Tissues Organs* **197**, 360, 2013.
5. MacBarb, R.F., Makris, E.A., Hu, J.C., and Athanasiou, K.A. A chondroitinase-ABC and TGF-beta1 treatment regimen for enhancing the mechanical properties of tissue-engineered fibrocartilage. *Acta Biomater* **9**, 4626, 2013.
6. DuRaine, G.D., Arzi, B., Lee, J.K., Lee, C.A., Responde, D.J., Hu, J.C., *et al.* Biomechanical evaluation of suture-holding properties of native and tissue-engineered articular cartilage. *Biomech Model Mechanobiol* **14**, 73, 2015.



7. Global Burden of Disease Study 2013 Collaborators. Global, regional, and national incidence, prevalence, and years lived with disability for 301 acute and chronic diseases and injuries in 188 countries, 1990–2013: a systematic analysis for the Global Burden of Disease Study 2013. *Lancet* **386**, 743, 2015.
8. Ofek, G., Revell, C.M., Hu, J.C., Allison, D.D., Grande-Allen, K.J., and Athanasiou, K.A. Matrix development in self-assembly of articular cartilage. *PLoS One* **3**, e2795, 2008.
9. DeLise, A.M., Fischer, L., and Tuan, R.S. Cellular interactions and signaling in cartilage development. *Osteoarthritis Cartilage* **8**, 309, 2000.
10. Tavella, S., Raffo, P., Tacchetti, C., Cancedda, R., and Castagnola, P. N-CAM and N-cadherin expression during in vitro chondrogenesis. *Exp Cell Res* **215**, 354, 1994.
11. Gigout, A., Jolicoeur, M., Nelea, M., Raynal, N., Farndale, R., and Buschmann, M.D. Chondrocyte Aggregation in suspension culture is GFOGER-GPP- and  $\beta 1$  integrin-dependent. *J Biol Chem* **283**, 31522, 2008.
12. Cao, L., Lee, V., Adams, M.E., Kiani, C., Zhang, Y., Hu, W., *et al.* Beta-integrin-collagen interaction reduces chondrocyte apoptosis. *Matrix Biol* **18**, 343, 1999.
13. Enomoto, M., Leboy, P.S., Menko, A.S., and Boettiger, D. Beta 1 integrins mediate chondrocyte interaction with type I collagen, type II collagen, and fibronectin. *Exp Cell Res* **205**, 276, 1993.
14. Hu, J.C., and Athanasiou, K.A. A self-assembling process in articular cartilage tissue engineering. *Tissue Eng* **12**, 969, 2006.
15. Mow, V.C., Gibbs, M.C., Lai, W.M., Zhu, W.B., and Athanasiou, K.A. Biphasic indentation of articular cartilage—II. A numerical algorithm and an experimental study. *J Biomech* **22**, 853, 1989.
16. Leitingner, B., McDowall, A., Stanley, P., and Hogg, N. The regulation of integrin function by  $Ca^{2+}$ . *Biochim Biophys Acta* **1498**, 91, 2000.
17. Brown, P.D., and Benya, P.D. Alterations in chondrocyte cytoskeletal architecture during phenotypic modulation by retinoic acid and dihydrocytochalasin B-induced reexpression. *J Cell Biol* **106**, 171, 1988.
18. Zhang, Z., Messana, J., Hwang, N.S., and Elisseeff, J.H. Reorganization of actin filaments enhances chondrogenic differentiation of cells derived from murine embryonic stem cells. *Biochem Biophys Res Commun* **348**, 421, 2006.
19. Rottmar, M., Mhanna, R., Guimond-Lischer, S., Vogel, V., Zenobi-Wong, M., and Maniura-Weber, K. Interference with the contractile machinery of the fibroblastic chondrocyte cytoskeleton induces re-expression of the cartilage phenotype through involvement of PI3K, PKC and MAPKs. *Exp Cell Res* **320**, 175, 2014.
20. Loty, S., Forest, N., Boulekbache, H., and Sautier, J.M. Cytochalasin D induces changes in cell shape and promotes in vitro chondrogenesis: a morphological study. *Biol Cell* **83**, 149, 1995.
21. Newman, P., and Watt, F.M. Influence of cytochalasin D-induced changes in cell shape on proteoglycan synthesis by cultured articular chondrocytes. *Exp Cell Res* **178**, 199, 1988.
22. Darling, E.M., Topel, M., Zauscher, S., Vail, T.P., and Guilak, F. Viscoelastic properties of human mesenchymally-derived stem cells and primary osteoblasts, chondrocytes, and adipocytes. *J Biomech* **41**, 454, 2008.
23. Woods, A., Wang, G., and Beier, F. RhoA/ROCK signaling regulates Sox9 expression and actin organization during chondrogenesis. *J Biol Chem* **280**, 11626, 2005.
24. Woods, A., Wang, G., Dupuis, H., Shao, Z., and Beier, F. Rac1 signaling stimulates N-cadherin expression, mesenchymal condensation, and chondrogenesis. *J Biol Chem* **282**, 23500, 2007.

Address correspondence to:  
Kyriacos A. Athanasiou, PhD, PE  
Department of Biomedical Engineering  
University of California, Davis  
One Shields Avenue  
Davis, CA 95616  
E-mail: athanasiou@ucdavis.edu

Soichiro Yamada, PhD  
Department of Biomedical Engineering  
University of California, Davis  
One Shields Avenue  
Davis, CA 95616  
E-mail: syamada@ucdavis.edu

Received: October 28, 2015  
Accepted: December 18, 2015  
Online Publication Date: January 26, 2016